Research Square

Preprints are preliminary reports that have not undergone peer review.
They should not be considered conclusive, used to inform clinical practice,
or referenced by the media as validated information.

Satellite gravimetric modeling to estimate magmatic sources in the Ometepe Island volcanic complex, Nicaragua

Darling F. Castro-Hidalgo
Universidad de Sonora
Christian R. Escudero
christian.escudero@academcios.udg.mx

Universidad de Guadalajara, Centro Universitario de la Costa

Research Article

Keywords: Ometepe Island, Concepción Volcano, Maderas Volcano, Gravimetric Anomalies

Posted Date: November 24th, 2026

DOI: https://doi.org/10.21203/rs.3.rs-11732125/v1

License: This work is licensed under a Creative Commons Attribution 4.0 International License.
Read Full License

Additional Declarations: No competing interests reported.

Satellite gravimetric modeling to estimate magmatic sources in the Ometepe Island volcanic complex, Nicaragua

Darling F. Castro-Hidalgo[1], Christian R. Escudero[2]

castrodarlingf@gmail.com https://orcid.org/0000-0002-9682-4391

christian.escudero@academcios.udg.mx https://orcid.org/0000-0002-2437-423X

[1]Universidad de Sonora, Hermosillo, Facultad de Ciencias Exactas y Naturales, Departamento de Geología, Sonora, México

[2]Universidad de Guadalajara, Centro Universitario de la Costa, Departamento de Ciencias Exactas, Centro de Estudios de la Tierra (CET), Puerto Vallarta, Jalisco, México

Corresponding author: Christian R. Escudero, christian.escudero@academcios.udg.mx

Abstract

To investigate the subsurface structure of the Ometepe Island volcanic complex in Nicaragua, we applied satellite gravimetric modeling using Global Gravity Model Plus data combined with high-resolution topography. We computed free-air, simple Bouguer, and complete Bouguer anomalies, applied terrain corrections using the orthogonal-grid prism method, and performed a 3D minimum-structure inversion. Our results reveal two distinct low-density bodies beneath the Concepción and Maderas volcanoes, with density contrasts of −0.10 to −0.05 g/cm³ relative to the surrounding densities, extending from shallow depths to approximately −2.0 km, and a high-density body (up to 0.15 g/cm³) on the northwestern flank of Concepción extending to −3.0 km. The low-density body beneath Maderas persists to greater depth than that beneath Concepción, suggesting a deeper and more persistent low-density source beneath the less active edifice. We conclude that the Ometepe Island volcanic complex is underlain by distinct shallow magmatic plumbing systems, with Concepción

exhibiting a shallow reservoir consistent with previous ground-based gravity studies, and Maderas retaining a deeper low-density structure from its earlier active phase.

Keywords: Ometepe Island, Concepción Volcano, Maderas Volcano, Gravimetric Anomalies

Resumen

Para investigar la estructura del subsuelo del complejo volcánico de la isla de Ometepe, en Nicaragua, aplicamos un modelado gravimétrico satelital con datos del modelo global de gravedad Plus, combinados con información topográfica de alta resolución. Calculamos las anomalías de aire libre, de Bouguer simple y de Bouguer completa; aplicamos correcciones topográficas mediante el método de prismas en una cuadrícula ortogonal, y realizamos una inversión 3D de estructura mínima. Los resultados revelan dos cuerpos distintos de baja densidad bajo los volcanes Concepción y Maderas, con contrastes de densidad de −0.10 a −0.05 g/cm³ respecto de las densidades circundantes. Estos cuerpos se extienden desde poca profundidad hasta aproximadamente −2.0 km. También identificamos un cuerpo de alta densidad (de hasta 0.15 g/cm³) en el flanco noroeste del Concepción, que se extiende hasta −3.0 km. El cuerpo de baja densidad bajo el Maderas llega a mayor profundidad que el situado bajo el Concepción, lo que sugiere la presencia de una fuente de baja densidad más profunda y persistente bajo el edificio volcánico menos activo. Concluimos que bajo el complejo volcánico de la isla de Ometepe hay sistemas someros de alimentación magmática distintos: el Concepción presenta un reservorio somero, en concordancia con estudios gravimétricos terrestres anteriores, mientras que el Maderas conserva una estructura profunda de baja densidad, remanente de una etapa previa de actividad.

Palabras clave: isla de Ometepe, volcán Concepción, volcán Maderas, anomalías gravimétricas

Introduction

Concepción Volcano is the most active composite volcano in Nicaragua and a key volcanic hazard on Ometepe Island, home to more than 31,000 inhabitants. Its frequent ash explosions are generally small to moderate, commonly VEI 1–2, but sufficient to sustain a summit pyroclastic cone and generate seasonal lahars that threaten settlements and agricultural areas around the volcano (Saballos et al., 2013). Because volcanic structure, magma storage, and conduit behavior strongly influence eruptive activity and instability, geophysical imaging of the volcano edifice is essential for hazard assessment (Saballos et al., 2013).

Gravity data are particularly useful in volcanic studies because they are sensitive to density contrasts between volcanic deposits, intrusions, faults, and possible shallow magma-related bodies. Satellite gravimetry has therefore become an essential tool for assessing magmatic systems and contributing to disaster risk reduction (Okubo, 2020), enabling detection of anomalies associated with subsurface density contrasts and helping define the internal geometry of volcanoes (Camacho et al., 2018). Many volcanic structures exhibit positive Bouguer anomalies associated with solidified, inactive magmatic bodies or plutonic intrusions, whereas negative anomalies are associated with active magmatic bodies containing magma less dense than the surrounding solid rock (Camacho et al., 2018; Sehah et al., 2023).

In Concepción, previous work has shown that the volcano is not a simple cone, but a complex edifice built in stages, with an older, denser truncated structure overlain by a younger, lower-density cone (Saballos et al., 2013). These earlier gravity and geodetic studies also suggested that continuous gravitational spreading alone does not fully explain the deformation and may instead reflect episodic volcanic or tectonic processes (Saballos et al.,

2013). Before this study, the shallow subsurface structure of Concepción Volcano was only partially constrained. Although ground-based gravity surveys had already revealed a bulk density of approximately 1764 ± 111 kg m^{-3}, a low-density upper cone, and possible concealed faults on the northeastern and southwestern flanks, the exact geometry of the volcanic interior and the relationship between gravity anomalies, magmatic plumbing, and structural discontinuities remained incompletely resolved (Saballos et al., 2013). Likewise, the interpretation of the volcano as actively spreading remained debated because GPS baselines did not provide clear evidence of continuous long-term extension, even though short-term recoverable deformation was observed during periods of unrest (Saballos et al., 2013).

This study investigates the subsurface structure of the Ometepe Island volcanic complex—with emphasis on Concepción and Maderas volcanoes—using satellite-derived gravimetric data. More specifically, this study builds on earlier gravity-based interpretations and assesses whether satellite-derived potential-field data can improve regional-scale characterization of the volcanic edifice and its plumbing system. Our approach uses the Global Gravity Model Plus (GGMplus; Hirt et al., 2013), which merges long-wavelength satellite gravity from GOCE/GRACE with high-frequency residual terrain corrections, providing effective detail at approximately 200 m scale. We computed free-air, simple Bouguer, and complete Bouguer anomalies, with terrain corrections applied using the orthogonal-grid prism method (Nagy, 1966; Nagy, 2000; Hammer, 1939). We then performed a 3D inversion of the complete Bouguer anomaly using Li and Oldenburg's (1998) minimum-structure approach, implemented in the open-source SimPEG framework (Cockett et al., 2015), to recover the three-dimensional distribution of density contrasts beneath the volcanic complex.

The Ometepec Island Volcanic System

Ometepec Island is located in the southwestern sector of Lake Nicaragua, within the Central American volcanic arc, and is constructed by two Quaternary stratovolcanoes, Concepción and Maderas, linked by a low-lying isthmus (Fig. 1; e.g., Borgia and van Wyk de Vries, 2003; Saballos et al., 2013; Scaini et al., 2012). Concepción (11.5°N, 85.6°W; ~1700 m.a.s.l.) forms the northwestern part of the island and is currently the most active composite volcano in Nicaragua, characterized historically by frequent Strombolian to sub-Plinian activity (VEI 1–2) and open-vent degassing (Borgia and van Wyk de Vries, 2003). Maderas (11.4°N, 85.5°W; ~1394 m.a.s.l.) forms the southeastern part of the island and is morphologically similar but presently much less active (Scaini et al., 2012). More than 30,000 inhabitants live on Ometepe and around the shores of Lake Nicaragua, making the volcanic complex a high-priority target for hazard assessment (Saballos, 2013; Scaini et al., 2012).

From a regional-tectonic perspective, Ometepec Island lies within the Nicaragua Depression, a forearc basin that developed above the subducting Cocos plate and is bounded to the southwest by the Rivas Anticline and related fault systems (Borgia and van Wyk de Vries, 2003). Seismic and geologic studies show that Ometepe is underlain by a thick (up to ~1 km) sequence of Quaternary lacustrine mudstones and volcaniclastic sediments filling the depression, overlying deformed Cretaceous–Paleogene marine and flysch formations (Rivas and Brito formations) and the Tertiary Coyol volcanic group exposed along the southwestern lake margin (Borgia and van Wyk de Vries, 2003). Within Lake Nicaragua, several major normal faults (San Ramón, Jesús María, Morrito, and the Lake Nicaragua fault zone) offset the basin floor and have been reactivated as oblique-slip structures accommodating forearc motion. Saballos et al. (2013) infer an additional N40°W-trending normal fault on the NE

flank of Concepción from sharp gravity gradients, interpreted as part of this regional fault network.

On Ometepec Island, surface geology is dominated by the edifices and deposits of Concepción and Maderas. Concepción is a steep cone built on lake sediments and lacustrine mudstones, with no significant pre-Concepción volcanic input recorded in the local sedimentary succession (Borgia and van Wyk de Vries, 2003). Its stratigraphy records at least four magmatic–eruptive episodes, including basaltic to dacitic Plinian and sub-Plinian eruptions (e.g., the Tierra Blanca Plinian phase at 2720 ± 60 yr B.P.) followed by construction of the modern summit pyroclastic cone and associated lava flows (Borgia and van Wyk de Vries, 2003; Kutterolf et al., 2007; Scaini et al., 2012). A topographic rise forming an annulus ~20 km in diameter around the cone has been interpreted as reflecting thrust-related folds and mud diapirs in the underlying lacustrine sequence, as well as localized uplift and deformation associated with volcanic spreading and substrata deformation (Borgia and van Wyk de Vries, 2003). These structural and stratigraphic relationships define strong lateral variations in density and elastic thickness that are critical for gravimetric modeling.

Existing ground-based gravity data provide important constraints on the density structure beneath Concepción and illustrate the type and scale of anomalies that satellite gravimetric modeling must resolve. Saballos et al. (2013) collected 206 gravity measurements over an ~18 × 12 km area covering the Concepción volcano, applied detailed terrain and Bouguer corrections, and derived a residual gravity field dominated by a pronounced low over the upper edifice and higher values on the lower flanks and surrounding plains. Using Nettleton and Parasnis' methods and subsequent adjustment to minimize correlation with topography, they estimated a bulk average density for the Concepción cone of 1764 ± 111 kg m^{-3}, substantially lower than the 2500–2700 kg m^{-3} previously assumed in

mechanical spreading models. The low gravity over the summit region is interpreted as reflecting a low-density summit pyroclastic cone, while the higher-density lower flanks are attributed to lava-dominated sequences (Saballos et al., 2013). Three-dimensional inversion of these data revealed an anomalous low-density body centered beneath Concepción at depths of ~1.7–2.1 km, interpreted as a shallow magmatic reservoir or highly fractured, volatile-rich zone (Saballos et al., 2013).

For satellite gravimetric modeling, Ometepec offers a compact, well-defined volcanic complex in which volcanic loads are emplaced on a relatively thin, low-density, mechanically weak sedimentary substratum within a structurally segmented basin. Concepción's low bulk density, pronounced summit gravity low, and localized deep anomalies at ~2 km depth provide a reference for validating satellite-derived anomalies against ground-based gravity and for testing inversion strategies that jointly resolve edifice and substratum contributions (Saballos et al., 2013). The presence of a second major edifice (Maderas) with distinct eruptive history and structural setting (Scaini et al., 2012), combined with the well-documented tephrostratigraphy and eruptive volumes along the Nicaraguan arc (Kutterolf et al., 2008), further allows regional evaluation of magmatic sources and density contrasts in a forearc environment where satellite gravimetric data can complement and extend sparse terrestrial surveys.

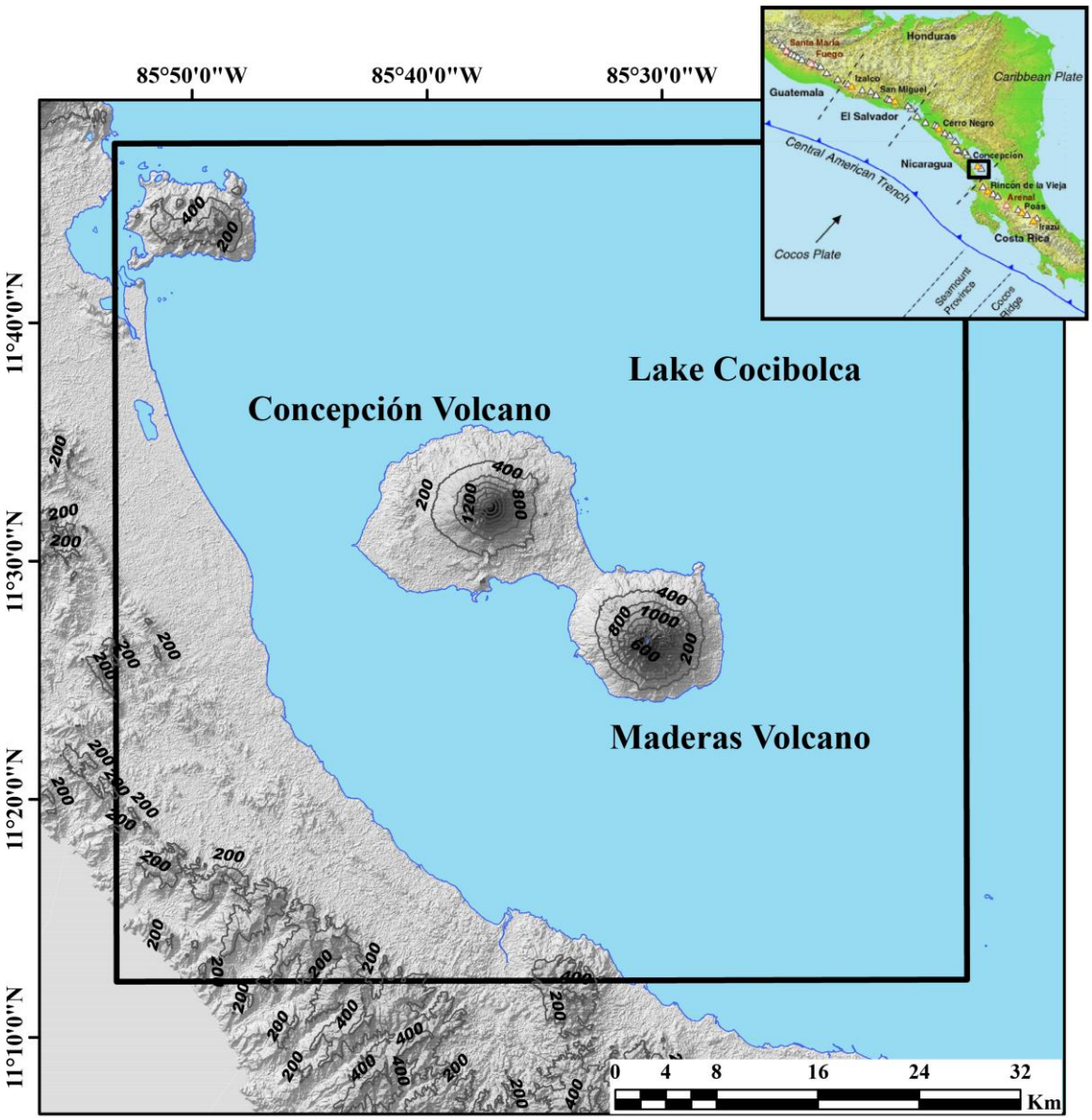

Fig 1. Location of Ometepec Island Volcanic Complex on the western side of Lake Cocibolca. Faults within the lake (SRFZ—San Ramon fault zone, JMFZ—Jesús María fault zone). Inset: Location map of Ometepec Island Volcanic System in Central America.

Materials and Method

Global Gravity Model Plus (GGMplus) is a composite gravity model that merges long-wavelength satellite gravity from GOCE/GRACE and EGM2008 with high-frequency residual terrain modeling (RTM), providing effective detail at ~200 m scale while preserving global consistency (Hirt et al., 2013). It delivers five gravitational-field products—free-air gravity acceleration, gravity disturbance from radial derivatives of the disturbing potential, north–south and east–west Helmert vertical deflections, and Molodensky quasi-geoid heights—with stated gravity-disturbance accuracy of 3–5 mGal over continental areas, improving where high-quality terrestrial gravity is available (Hirt et al., 2013). These characteristics make the model suited to delineating crustal structures, estimating source depths, and mapping density contrasts in regions where terrestrial gravity is sparse, costly, or logistically difficult to acquire.

In volcanic settings, GGMplus resolves shallow structures (<10 km depth) more sharply than coarser models such as EIGEN-6C4, which remain better suited to deeper regional sources (Alvarez and Camacho, 2023, 2025). The model has been applied successfully to geothermal and fault-structure mapping, where derivative analysis and 3D inversion have identified shallow clay caps, deeper reservoir layers, and mass deficits consistent with magmatic sources (Soekarno et al., 2025; Sehah et al., 2023; Lase et al., 2025), and comparisons with land gravity surveys show close agreement in residual anomalies, confirming its capacity to fill spatial gaps in ground coverage (Wiguna et al., 2024). Its principal limitation is that the "ultrahigh resolution" derives partly from RTM, so short-wavelength anomalies may reflect topography rather than subsurface density structure, particularly in steep terrain (Ananda et al., 2025). For the Ometepe volcanic complex, where

rugged relief and limited terrestrial coverage preclude dense ground surveying, this trade-off is acceptable provided terrain effects are treated explicitly. GGMplus therefore supplies the spatially dense, high-resolution framework required to construct Bouguer anomaly maps, isolate short-wavelength anomalies associated with shallow bodies and feeder zones, separate regional trends, and constrain 2D/3D inversion of magmatic sources and the structures controlling magma ascent.

We obtained the GGMplus 2013 gravity grids through the public distribution portals maintained by the Bureau Gravimétrique International and the Curtin University GGMplus server (Hirt et al., 2013). GGMplus provides five gravitational-field products at the Earth's surface; of these, we selected the gravity perturbation function (*dg*), which represents the difference between observed gravity and normal gravity at the same reference point on the topographic surface. Because it already incorporates the free-air correction, this product is equivalent to the free-air anomaly and serves directly as the input for the Bouguer reduction (Ananda et al., 2025; Hirt et al., 2013). We adopted it as the starting field for the processing workflow, following the practice established in recent volcanic and geothermal applications of GGMplus (Alvarez and Camacho, 2023, 2025; Soekarno et al., 2025; Lase et al., 2025; Sehah et al., 2023), because it retains both long- and short-wavelength signals and is delivered at the native model resolution.

Data and Pre-processing

We used the GGMplus 2013 gravity grids, distributed by the Bureau Gravimétrique International and the Curtin University GGMplus server (Hirt et al., 2013). Of the five gravitational-field products available, we selected the gravity disturbance (*dg*) — the difference between observed and normal gravity at the same point on the topographic surface — because it already incorporates the free-air correction and therefore approximates the free-

air anomaly, allowing it to serve directly as input to the Bouguer reduction (Ananda et al., 2025). This choice follows recent volcanic and geothermal applications of GGMplus (Alvarez and Camacho, 2023, 2025; Sehah et al., 2023; Soekarno et al., 2025; Lase et al., 2025).

Grids were extracted over a rectangular window extending at least 10–20 km beyond the volcanic edifice in all directions, preserving the native 7.5″ spacing. They were then projected to UTM zone 16N and resampled by bilinear interpolation onto a regular grid of $\Delta x \approx \Delta y \approx 0.2–0.25$ km. No data voids occurred over the island; to suppress edge artifacts during filtering and continuation, the domain was padded by mirroring the outermost 5–10 cells.

Bouguer anomalies

Theoretical gravity was computed at each node using the GRS80 formula (Moritz, 2000):

$$\gamma(\varphi) = \gamma_e \frac{1 + k sin^2 \varphi}{\sqrt{1 - \mathrm{e}^2 \sin^2 \varphi}},$$

where γ_e is equatorial gravity, k is the normal-gravity coefficient, and e is the first eccentricity of the ellipsoid. Free-air anomalies obtained from dg using the standard vertical gradient of 0.3086 mGal m^{-1} agreed with the GGMplus free-air product to within ∼1 mGal, confirming consistency of the implementation.

A reduction density of 2.20×10^3 kg m^{-3} was determined for the study area from the Nettleton and Parasnis methods (Nettleton, 1939; Parasnis and Cook, 1952), using equivalent thicknesses derived from the DEM ALOS PALSAR (12.5 meters per pixel) referenced to WGS84 (Li and Götze, 2001). Simple Bouguer anomalies were obtained by subtracting the slab correction

$$\delta g_{slab} = 2\pi G \rho h,$$

from the free-air anomaly, where h is elevation, and G is the gravitational constant (Hinze et al., 2005).

Because GGMplus includes topography only implicitly through residual terrain modeling, we recomputed the terrain correction explicitly, using the orthogonal-grid prism method (Hammer, 1939; Nagy, 1966; Nagy et al., 2000). Topography around each node was discretized into right rectangular prisms with a density of 2.20×10^{3} kg m^{-3}, and the vertical attraction of each prism was evaluated using Nagy's (2000) closed-form expression. Contributions were summed within an integration radius of 3 km. The correction is positive irrespective of whether the surrounding relief lies above or below the station. Adding it to the simple Bouguer anomaly yielded the complete Bouguer anomaly.

3.3. Three-dimensional inversion

Density contrasts were recovered by minimum-structure inversion of the residual complete Bouguer anomaly (Li and Oldenburg, 1998). The subsurface was discretized into a rectilinear mesh of 82 × 82 × 46 cells that extended ~51.6 km laterally (approximately ±25.8 km from the center) and to ~28.3 km depth below the maximum topography, with cell size increasing from 500 m beneath the edifice (expansion factor of 1.3 in the padding cells). Topography was embedded in the mesh, and cells above the surface were assigned zero density contrast.

The forward operator evaluates the vertical attraction of each prism using the analytical expression of Nagy (2000). Regularisation followed a Tikhonov scheme that balanced a weighted data-misfit term against a model objective function penalizing deviation from a zero-contrast reference model and first-order spatial roughness. A depth-weighting function $w(z) \propto (z + z_0)^{-2}$ counteracted the decay of sensitivity with depth (Li and Oldenburg, 1998). No box constraints were applied to the density contrasts. Inversion used the open-source SimPEG framework (Cockett et al., 2015), with an inexact Gauss–Newton optimizer

(maxIter = 4000, maxIterLS = 20, maxIterCG = 10, tolCG = 1×10^{-2}); the trade-off parameter was adjusted iteratively until the χ^2 misfit was consistent with the assigned per-datum uncertainties ($\sigma \approx 0.93$ mGal, set as 2% of the maximum observed anomaly of 46.71 mGal), and a matrix-free solver avoided explicit storage of the full sensitivity matrix.

Results

To identify heterogeneous structures and evaluate the composition and distribution of subsurface masses in the volcanic complex of Ometepe Island, we estimated gravimetric anomalies and relative density contrasts from satellite-derived GGMplus gravity data. The complete Bouguer anomaly and subsequent 3D inversion reveal two low-density bodies beneath the Concepción and Maderas volcanoes, extending from shallow depths to approximately −2.0 km, and a high-density body on the northwestern flank of Concepción extending to −3.0 km. These results help establish a subsurface structural model that improves understanding of the volcanic-tectonic evolution of the study area.

Gravimetric Anomalies

To characterize the regional gravity field and its relationship to surface topography, we computed free-air, simple Bouguer, and complete Bouguer anomalies from the GGMplus gravity disturbances. The resulting anomaly maps (Fig. 2) reveal distinct patterns that correlate with the volcanic edifices and surrounding lowlands.

The orthometric height model (Fig. 2a) shows elevations ranging from less than 100 m above sea level in the lowlands surrounding the volcanoes to a maximum of approximately 1,200 m above sea level at the summits of Concepción and Maderas. This altitudinal variation is directly reflected in the free-air gravity anomalies (Fig. 2b), which are strongly influenced by topographic changes. The low-elevation areas adjacent to Lake Cocibolca recorded values

around 10 mGal, indicating a mass deficit associated with the lake body and unconsolidated sedimentary fill. In contrast, the high-altitude zones of the volcanic edifices show a significant increase in gravity, reaching up to 100 mGal, corresponding to a mass excess associated with the volcanic piles.

The simple Bouguer anomaly (Fig. 2c), computed using a reduction density of 2.20 g/cm³, reveals a pronounced negative anomaly below −10 mGal beneath both the Concepción and Maderas volcanic structures. This negative anomaly is interpreted as reflecting low-density pyroclastic deposits and fractured volcanic materials that comprise the upper portions of the edifices. Conversely, a positive anomaly of approximately 50 mGal is observed in the peripheral sector surrounding the volcanic complex, which we attribute to denser basement rocks or older volcanic sequences. These patterns are more clearly highlighted in the complete Bouguer anomaly (Fig. 2d), which incorporates explicit terrain corrections using the orthogonal-grid prism method. The complete Bouguer anomaly highlights the negative anomalies beneath the volcanoes and enhances the contrast with the positive anomalies in the surrounding lowlands, confirming that the volcanic edifices are underlain by lower-density material than the regional basement.

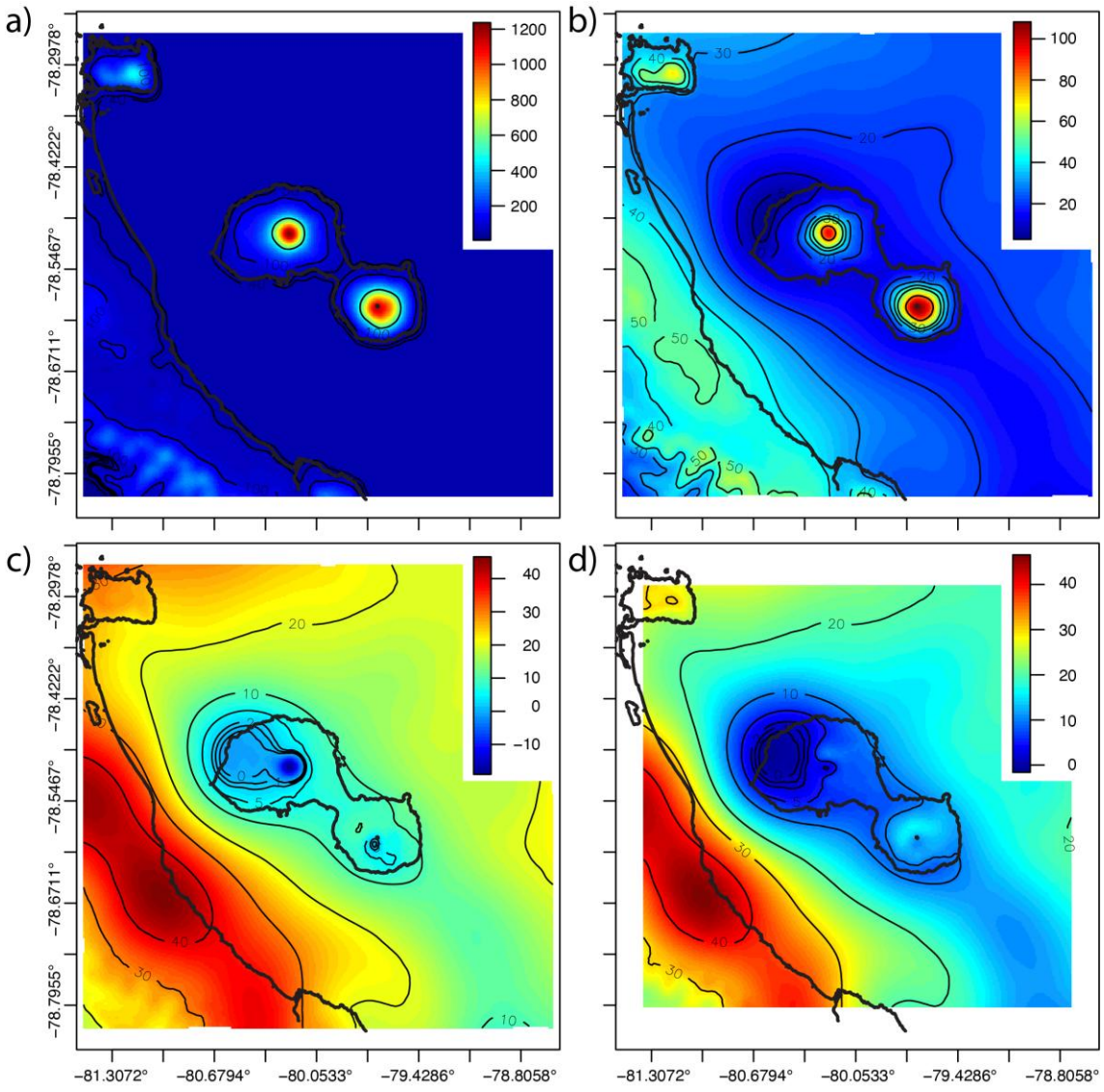

Fig. 2 Gravimetric anomalies: a) orthometric height, equivalent to the ALOS PALSAR WGS84 elevation model with 12 m resolution; b) GGMplus free-air anomalies, obtained from the difference between theoretical gravity and the elevation correction; c) Simple Bouguer Anomaly, computed by subtracting the free-air anomalies from the observed gravity using an average density of 2.20 g/cm³; and d) Complete Bouguer Anomaly, determined by applying the terrain correction using an orthogonal grid.

Density Contrast Inversion

To determine the three-dimensional distribution of subsurface density contrasts, we performed a 3D inversion of the complete Bouguer anomaly using the minimum-structure approach of Li and Oldenburg (1998), implemented in the SimPEG framework (Cockett et al., 2015). The inversion recovers relative density contrasts (χ) with respect to a zero-density reference model, with negative values indicating low-density bodies and positive values indicating high-density bodies.

The inverted density contrast maps at selected depths (Fig. 3) reveal the spatial distribution of anomalous bodies beneath the volcanic complex. At shallow depths (z = 0.1 to −0.5 km; Figs. 3a–c), two distinct low-density bodies are clearly resolved, with contrasts of −0.10 to −0.05 g/cm^3 relative to the surrounding densities. The first low-density body is located beneath the northern sector of Concepción volcano (approximately x = −5, y = 5) and exhibits a roughly circular geometry. The second is situated in the north-south sector of Maderas volcano (approximately x = 10, y = 5) and displays an elliptical shape elongated along the volcano's axis. These low-density bodies persist to intermediate depths (z = −1.0 to −2.0 km; Figs. 3d–e), maintaining their general geometries but gradually decreasing in intensity.

At depths of −1.0 km and deeper (Figs. 3d–f), a high-density body with contrasts of up to 0.15 g/cm^3 becomes apparent in the northwest region of Concepción volcano, extending from x = −5 to x = −15 and y = −5 to y = 15. This positive anomaly is interpreted as a dense intrusive body or a solidified magmatic core. Notably, the low-density body beneath Maderas volcano persists to a depth of −3.0 km (Fig. 3f), suggesting a deeper and more persistent low-density source beneath this edifice

compared to Concepción. At depths below −3.0 km, the low-density anomalies are no longer resolved, indicating that the magmatic sources are confined to the upper crust and give way to denser basement rocks.

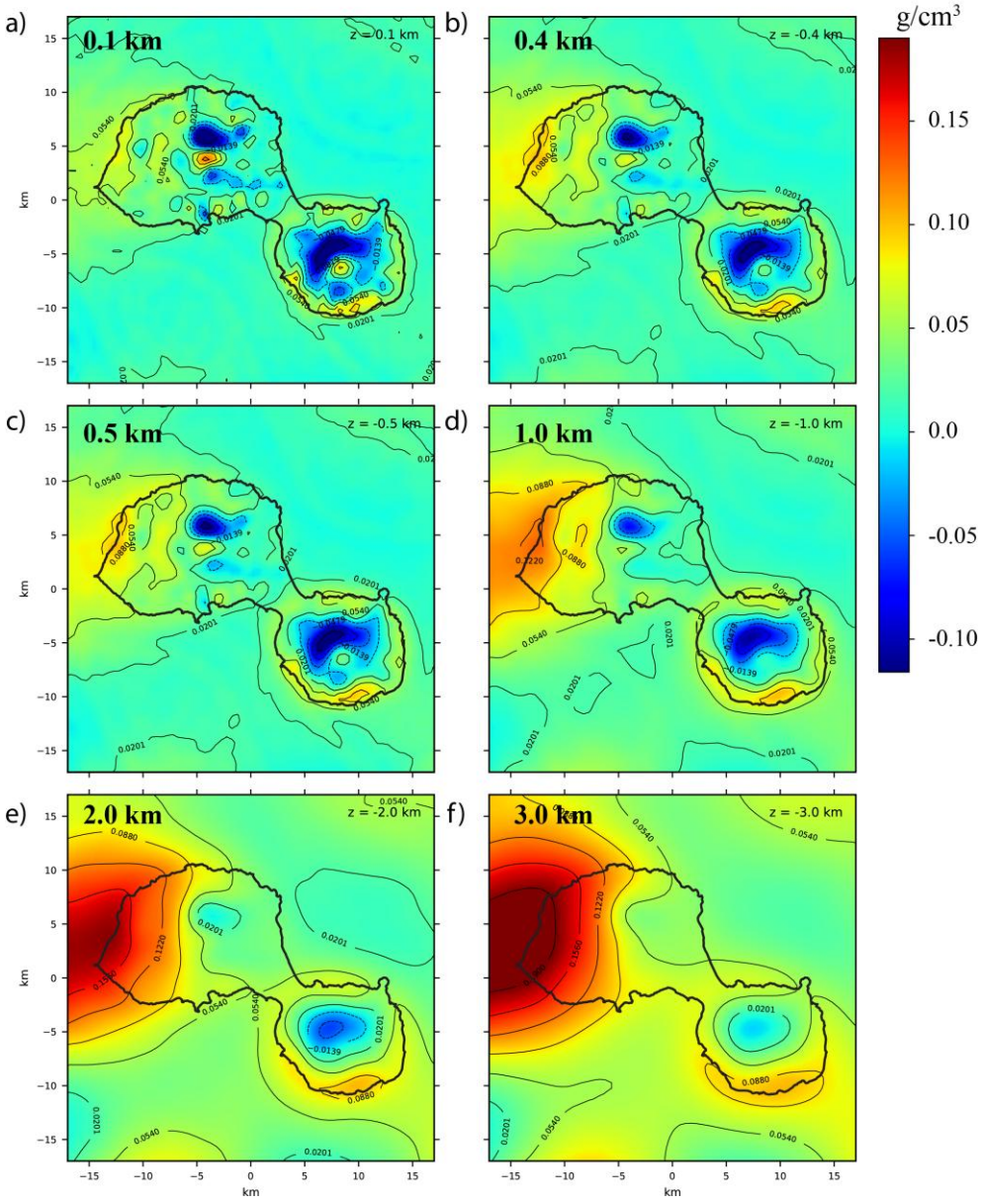

Fig. 3 Density contrast maps at various depths: a) 0.1 km, b) 0.4 km, c) 0.5 km, d) 1.0 km, e) 2.0 km, f) 3.0 km. Negative values (blue to green) represent low densities (−0.10 to −0.05 g/cm³), while positive values (orange to red) represent high densities (0.10 to 0.15 g/cm³). The black line delineates the Ometepe Island Volcanic Complex.

Discussion and Conclusion

The gravity anomaly maps (Fig. 2) reveal a close relationship between the regional gravity response and the volcanic morphology of the Ometepe Island complex. The free-air anomaly shows localized maxima coinciding with the volcanic edifices of Concepción and Maderas, primarily reflecting topography and the mass concentration associated with the volcanic cones. However, after applying Bouguer corrections, the gravity signal reveals features more representative of the density distribution at depth. The complete Bouguer anomaly shows a broad positive regional anomaly reaching values close to 50 mGal in the western and southwestern sectors of the study area, which we attribute to the regional structure defined by the Tertiary anticline of the Rivas Formation, located northwest of Lake Cocibolca. In contrast, the volcanic complex shows a negative Bouguer anomaly of approximately −10 mGal, indicating a relative mass deficit beneath the volcanic edifices. This behavior is consistent with observations from other volcanic systems, where low-density zones are associated with accumulations of partially melted magma, hydrothermal complexes, highly fractured pyroclastic sequences, or hydrothermally altered rocks (Camacho et al., 2018; Sehah et al., 2023).

The 3D gravity inversion reinforces this interpretation. Density contrast maps reveal two main low-density bodies, with values ranging between −0.10 and −0.05 g/cm³ relative to the surrounding density. These negative anomalies are clearly observed at shallow depths (z = 0.1 to −1.0 km) beneath both volcanic edifices. The body associated with Concepción Volcano is located in the northern sector of the volcanic structure (x ≈ −5 km, y ≈ 5 km) and exhibits a roughly circular geometry. Due to the historical and current activity of this volcano, we interpret this anomaly as a shallow magmatic reservoir or a transient magma storage zone

363 that feeds recent eruptive processes. This interpretation aligns with the gravity-based
364 discovery of Saballos et al. (2013), who identified a pronounced residual gravity low beneath
365 the upper edifice and an anomalous mass centered at approximately 2 km depth beneath
366 Concepción. The consistency between our satellite-derived results and Saballos' ground-
367 based gravity findings is notable: both approaches resolve a low-density body at comparable
368 depths (1.7–2.2 km in Saballos' inversion; 1.0–2.0 km in our model), supporting the
369 interpretation of a shallow magmatic source region beneath the active edifice.

370 Meanwhile, Maderas Volcano exhibits a more extensive negative anomaly distributed
371 in a north-south direction ($x \approx 10$ km, $y \approx 5$ km). Unlike the structure beneath Concepción,
372 this body maintains continuity down to depths near −3.0 km, suggesting greater volume and
373 persistence. Given that Maderas is an older, currently inactive edifice (Scaini et al., 2012),
374 this anomaly likely reflects remnants of previous magmatic storage systems that favor
375 preserving lower-density materials, such as highly fractured or hydrothermally altered rocks.
376 This deeper persistence beneath the less active volcano is unexpected. While both volcanoes
377 exhibit low-density anomalies, their contrasting depth extents imply different construction
378 histories and magmatic evolution. The deeper anomaly beneath Maderas may indicate a more
379 extensive plumbing system that has since cooled and fractured, or a larger volume of low-
380 density cumulate material remaining from its active phase.

381 A notable feature of the model is the presence of a high-density body with contrasts
382 reaching approximately 0.15 g/cm³ in the northwest sector of Concepción Volcano,
383 extending from $x = -15$ km to $x = -5$ km and from $y = -5$ km to $y = 15$ km, consistently
384 observed between −1.0 and −3.0 km depth. The geometry and continuity of this anomaly
385 suggest denser materials than the surrounding volcanic environment, possibly associated
386 with the consolidated volcanic basement or a dense intrusive core. The spatial coincidence

between this high-density body and the positive Bouguer anomaly in the western sector supports a connection with the Tertiary anticline of the Rivas Formation, consistent with the regional tectonic framework described by Borgia and van Wyk de Vries (2003). This high-density body may represent the subsurface expression of the Rivas Anticline or an associated intrusive complex that reinforces the western flank of the edifice.

Comparison with previous GGMplus volcanological studies reveals both consistencies and methodological advantages. Previous work showed that GGMplus offers superior spatial resolution for shallow volcanic structures (<10 km depth) than EIGEN-6C4, with sharper delineation of low-density volcanic bodies. Alvarez and Camacho (2023, 2025) successfully used GGMplus-derived Bouguer anomalies to image upper-crustal magma chambers beneath Popocatépetl and Iztaccíhuatl, and to resolve near-surface density variations in the Hunga Tonga–Hunga Ha'apai island arc setting. Our results are consistent with these findings: the low-density bodies beneath Concepción and Maderas (0 to −3.0 km depth, −0.10 to −0.05 g/cm³ contrasts) fall within the same order of magnitude as those resolved in these studies. However, unlike many GGMplus applications that lack independent ground-truthing, our Ometepe study benefits from high-quality ground-based gravity data (Saballos et al., 2013) that validate the satellite-derived anomalies. The 3D inversion of Saballos' ground data revealed a bulk density of 1764 ± 111 kg m^{-3} for Concepción's edifice and an anomalous mass centered at ~1.7–2.1 km depth, consistent with our interpretation of a shallow magmatic reservoir. This consistency strengthens confidence in the GGMplus approach for volcanic imaging in remote or rugged terrains.

However, limitations must be acknowledged. As Hirt et al. (2013) and Ananda et al. (2025) emphasize, GGMplus's "ultrahigh resolution" is partly derived from residual terrain modeling (RTM), meaning the model contains a strong topographic component that can

411 mimic geologic detail but does not directly represent subsurface density structure. In steep
412 volcanic terrain like Ometepe, topography-driven signals may be overinterpreted as
413 magmatic or tectonic features. To mitigate this, we explicitly recomputed terrain corrections
414 using the orthogonal-grid prism method (Nagy, 1966, Hammer, 1939), consistent with best
415 practices in recent GGMplus studies (Lase et al., 2025). Nevertheless, some residual
416 topographic signal may remain in the inversion. Additionally, our inversion depth estimates
417 are subject to non-uniqueness inherent to potential-field methods, despite the application of
418 depth weighting following Li and Oldenburg (1998). The density contrasts recovered
419 represent relative values with respect to the reference model; absolute densities would require
420 additional petrophysical constraints.

421 A second limitation concerns the bulk reduction density used in this study (2.20
422 g/cm³), which differs from Saballos' bulk edifice density (1.76 g/cm³). This difference is not
423 contradictory but reflects different target volumes: Saballos' value refers specifically to the
424 upper volcanic edifice—essentially a pile of tephra and pyroclastic material—whereas our
425 2.20 g/cm³ corresponds to the broader volcanic-and-sedimentary package used for Bouguer
426 reduction across the entire island and surrounding lake, including denser lava flows and
427 underlying basement. This distinction should be considered when comparing density values
428 between studies.

429 The volcanic complex is situated above a regional higher-density structure (the Rivas
430 Anticline), while lower-density materials predominate beneath the volcanic edifices. This
431 distribution is consistent with a shallow magmatic reservoir beneath Concepción Volcano
432 and a deeper low-density structure beneath Maderas Volcano. Our results demonstrate that
433 satellite gravimetric data can effectively complement ground-based geophysical surveys,
434 particularly in remote island settings where terrestrial gravity coverage is limited. For the

Ometepe Island volcanic complex, the results provide new constraints on the geometry of magmatic sources and their relationship to surface morphology, improving hazard assessment and our understanding of the region's volcanic-tectonic evolution.

This study's findings have several important implications. First, they show that GGMplus satellite gravity data, combined with rigorous terrain correction and 3D inversion, offer a cost-effective, spatially comprehensive approach to imaging magmatic systems in remote or rugged volcanic terrains. This is particularly relevant for volcanic hazard assessment in regions where ground-based geophysical surveys are logistically challenging or prohibitively expensive. Second, detecting two distinct low-density bodies beneath Concepción and Maderas, with contrasting depth extents, provides new insights into the volcanic evolution of the Ometepe complex. The deeper anomaly beneath the older, less active Maderas Volcano suggests that even dormant edifices can retain substantial low-density volumes, with implications for edifice stability and potential reactivation. Third, identifying a high-density body on the northwestern flank of Concepción, possibly linked to the Rivas Anticline, highlights how regional tectonic structures control volcanic system architecture. Future hazard models should incorporate these structural controls. More broadly, this study shows that satellite gravimetry can bridge the gap between sparse field measurements and regional-scale interpretations, providing a valuable framework for volcanic and tectonic studies in the Central American arc and analogous settings worldwide.

Author Contributions Darling F. Castro-Hidalgo: Conceptualization, Data curation, Formal analysis, Investigation, Methodology, Writing – original draft. Christian R. Escudero: Supervision, Methodology, Validation, Visualization, Writing – review and editing.

Funding No particular source of funding was utilized.

Data and Resources All GGMplus 2013 data supporting the findings of this study is available via the public distribution portal maintained by the Bureau Gravimétrique International (BGI; https://bgi.obs-mip.fr) and the Curtin University GGMplus server (Hirt et al., 2013).

Declarations

Competing interest The authors declare no competing interests.

References

Alvarez R, Camacho M (2023) Plumbing system of Hunga Tonga Hunga Ha'apai volcano. *J Earth Sci* 34:706–716. https://doi.org/10.1007/s12583-022-1792-0

Alvarez R, Camacho-Ascanio M (2025) Gravimetric definition of the magmatic chambers of the Popocatépetl-Iztaccíhuatl volcanic complex, Mexico. *Earth Sci Eng*. https://doi.org/10.57237/j.earth.2025.01.001

Ananda R, Arisbaya I, Grandis H (2025) The GGMPlus global gravity data from the geophysical exploration perspective. *IOP Conf Ser: Earth Environ Sci* 1458:012041. https://doi.org/10.1088/1755-1315/1458/1/012041

Borgia A, van Wyk de Vries B (2003) The volcano-tectonic evolution of Concepción, Nicaragua. *Bull Volcanol* 65:248–266. https://doi.org/10.1007/s00445-002-0256-8

Camacho AG, Prieto JF, Ancochea E, Fernández J (2018) Deep volcanic morphology below Lanzarote, Canaries, from gravity inversion: new results for Timanfaya and implications. *J Volcanol Geotherm Res* 369:64–79. https://doi.org/10.1016/j.jvolgeores.2018.11.013

480 Cockett R, Kang S, Heagy LJ et al (2015) SimPEG: an open source framework for simulation
481 and gradient based parameter estimation in geophysical applications. *Comput Geosci*
482 85:142–154. https://doi.org/10.1016/j.cageo.2015.09.015

483 Hammer S (1939) Terrain corrections for gravimeter stations. *Geophysics* 4:184–194.
484 https://doi.org/10.1190/1.1440495

485 Hinze WJ, Aiken C, Brozena J, Coakley B, Dater D, Flanagan G, Forsberg R, Hildenbrand
486 T, Keller GR, Kellogg J, Kucks R, Li X, Mainville A, Morin R, Pilkington M, Plouff D,
487 Ravat D, Roman D, Urrutia-Fucugauchi J, Winester D (2005) New standards for reducing
488 gravity data: the North American gravity database. *Geophysics* 70:J25–J32.
489 https://doi.org/10.1190/1.1988183

490 Hirt C, Claessens S, Fecher T et al (2013) New ultrahigh-resolution picture of Earth's gravity
491 field. *Geophys Res Lett* 40:4279–4283. https://doi.org/10.1002/grl.50838

492 Kutterolf S, Freundt A, Pérez W (2008) Pacific offshore record of plinian arc volcanism in
493 Central America: 2. Tephra volumes and erupted masses. *Geochem Geophys Geosyst* 9.
494 https://doi.org/10.1029/2007GC001791

495 Lase FTZ, Aprina PU, Ferucha I, Alawiyah S (2025) Modelling of heat source in the
496 geothermal field based on Euler deconvolution and Occam inversion using GGMPlus
497 gravity data. *IOP Conf Ser: Earth Environ Sci* 1547:012012.
498 https://doi.org/10.1088/1755-1315/1547/1/012012

499 Li X, Götze H-J (2001) Ellipsoid, geoid, gravity, geodesy, and geophysics: correctly
500 understanding gravity. *Geophysics* 66:1660–1668. https://doi.org/10.1190/1.1487109

501 Li Y, Oldenburg DW (1998) 3-D inversion of gravity data. *Geophysics* 63:109–119.
502 https://doi.org/10.1190/1.1444302

503 Moritz H (2000) Geodetic Reference System 1980. *J Geodesy* 74:128–133.
504 https://doi.org/10.1007/s001900050278

505 Nagy D (1966) The prism method for terrain corrections using digital computers. *Pure Appl*
506 *Geophys* 63:31–39. https://doi.org/10.1007/BF00875156

Nagy D, Papp G, Benedek J (2000) The gravitational potential and its derivatives for the prism. *J Geodesy* 74:552–560. https://doi.org/10.1007/s001900000116

Nettleton LL (1939) Determination of density for reduction of gravimeter observations. *Geophysics* 4:176–183. https://doi.org/10.1190/1.1437088

Okubo S (2020) Advances in gravity analyses for studying volcanoes and earthquakes. *Proc Jpn Acad Ser B* 96:50–69. https://doi.org/10.2183/pjab.96.005

Parasnis DS, Cook AH (1952) A study of rock densities in the English Midlands. *Geophys Suppl Mon Not R Astron Soc* 6:252–271. https://doi.org/10.1111/j.1365-246X.1952.tb03013.x

Saballos JA, Malservisi R, Connor CB (2013) Gravity and geodesy of Concepción Volcano, Nicaragua. In: *Understanding open-vent volcanism and related hazards*. Geological Society of America Special Paper 498. https://doi.org/10.1130/2013.2498(05)

Scaini C, Folch A, Navarro M (2012) Tephra hazard assessment at Concepción Volcano, Nicaragua. *J Volcanol Geotherm Res* 219:41–51. https://doi.org/10.1016/j.jvolgeores.2012.01.007

Sehah S, Koesuma S, Prabowo UNW, Ikhwana AZ (2023) Utilization of satellite gravimetric data to estimate the location of the magma chamber of Slamet volcano, Central Java, Indonesia. *Indones J Appl Phys* 13:241–251. https://doi.org/10.13057/ijap.v13i2.73923

Soekarno H, Pranoto B, Restiana A et al (2025) Identifying geological fault structures using GGMplus satellite data and derivative methods to characterize Mount Endut geothermal systems via 3D-inversion gravity modeling. *Geomat Environ Eng* 19:31–62. https://doi.org/10.7494/geom.2025.19.3.31

Wiguna IPAP, Rosid MS, Saputra FRT (2024) Comparison of land surface and GGMPlus satellite gravity data results (case study: the Kalibening Basin). *J Penelit Pendidik IPA* 10:4579–4588. https://doi.org/10.29303/jppipa.v10i8.7318